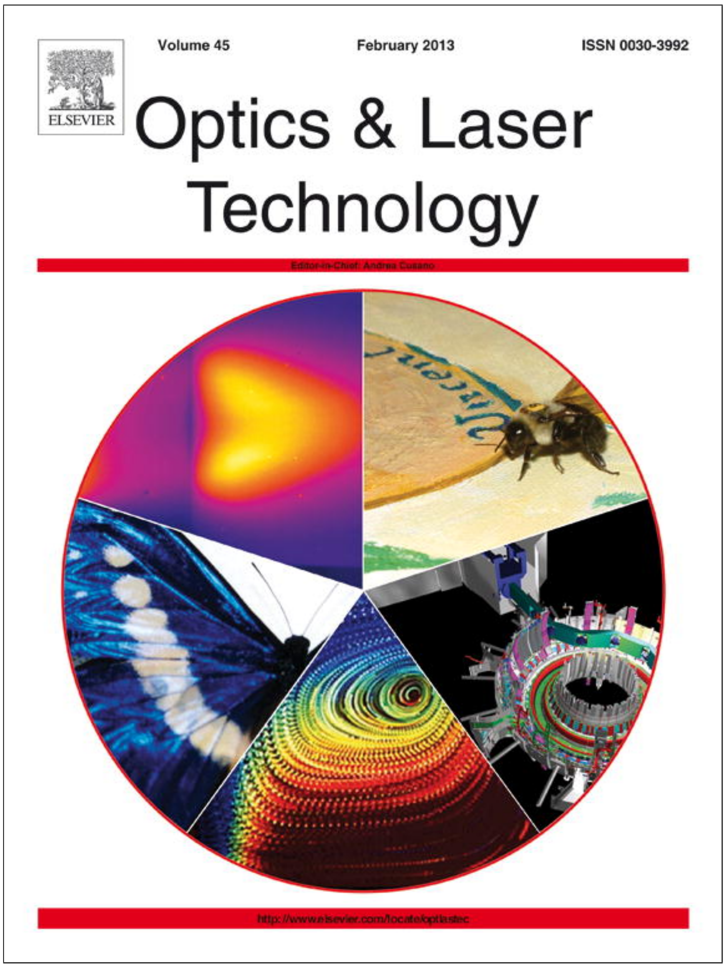
Volume 45
February 2013
ISSN 0030-3992
ELSEVIER
Optics & Laser Technology

Optics & Laser Technology 45 (2013) 495–502

Contents lists available at SciVerse ScienceDirect

Optics & Laser Technology

journal homepage: www.elsevier.com/locate/optlastec

Effect of focusing conditions and laser parameters on the fabrication of gold nanoparticles via laser ablation in liquid

Khaled A. Elsayed [a,*], Hisham Imam [b], M.A. Ahmed [a], Rania Ramadan [a]

[a] Materials Science Laboratory(1), Physics Department, Faculty of Science, Cairo University, Giza 12211, Egypt
[b] National Institute of Laser Enhanced Sciences, Cairo University, Giza 12211, Egypt

ARTICLE INFO

Article history:
Received 19 March 2012
Received in revised form
5 June 2012
Accepted 6 June 2012
Available online 28 June 2012

Keywords:
Gold nanoparticles
Laser ablation
Absorbance spectrum
Focusing conditions

ABSTRACT

The generation of nanoparticles using pulsed laser ablation has inherent advantages compared to conventional methods, like the purity and stability of the fabricated nanoparticles, aerosols and colloids. This study addresses the influence of laser parameters such as laser fluence, laser wavelength as well as focusing condition of laser beam on the size and morphology of the gold nanoparticles prepared in de-ionized water by pulsed laser ablation. The optimum conditions at which gold nanoparticles are obtained with controllable average size have been reported as these parameters affected the size, distribution and absorbance spectrum. The effect of laser fluence was studied. The laser fluences were divided into three regions (low, middle and high). A noteworthy change was observed at each region. At low fluences, the size of the nanoparticles decreases as the fluence increases to a certain critical value after which the size of the nanoparticles increases as the fluence increases. Also a significant change in the size distribution of the gold nanoparticles was noticed during the variation of the focusing conditions at gold–water interface.

1. Introduction

In the last few years and due to unique physicochemical characteristics of gold nanoparticles and their wide usages in different fields, the number of publications on the preparation and characterization of gold nanoparticles have extensively increased [1,2]. The ability of gold to produce heat after absorbing light provides a medicinal usage named as photothermal therapy [3]. Hazardous effects of organic solvents, reducing agents and toxic reagents applied for synthesis of gold nanoparticles on environment, encouraged researchers to develop simple and safe methods for preparation of gold nanoparticles [4,5].

Conventional nanoparticle generation routes such as mechanical milling and grinding, or chemical generation methods like the sol–gel process show drawbacks related to the purity and variety of accessible materials. Different nanoparticulate materials are already used for a variety of applications such as bio-imaging, antiseptic metal ion release, cancer treatment, UV-protection, photo-catalytic effects, scratch-resistance and corrosion protection [6]. But the availability of nanoparticles with high purity is still lacking in particular for biomedical applications [7,8].

Pulsed laser ablation is an alternative method addressing the deficits of the conventional methods. It offers the access to an unlimited nanomaterial spectrum, since the nanoparticles may be generated from almost any solid material [9–11]. Advantages of this method include the relative simplicity of the procedure and the absence of chemical reagents in the final preparation, high purity of the nanomaterial, the material variety, and the in-situ dispersion of the nanoparticles in a variety of liquids allowing safe and stable handling of the colloids but the size distributions of the gold nanoparticles prepared by this technique tend to be broadened due to the agglomeration and ejection of large fragments during laser ablation. However, there is still a lack of data about the influences of focusing conditions on the size of the generated nanoparticles.

The number of publications on laser ablation and nanoparticles generation in liquid increased intensively in the last decade. A nearly unlimited combination of nanoparticulate material, liquid medium and conjugative agents allow the fabrication of a huge variety of collides with extensively high purity which are required in many applications especially biomedicine [12]. Intensive research is being carried out to understand the main factors affecting the formation mechanism of nanoparticle from laser ablated material [13–15].

The control of the gold nanoparticles size and hence colloidal properties is possible using laser parameters such as laser fluence and wavelength as well as varying the focusing conditions. In this study, these parameters that affect the particle size distribution of the gold nanoparticle prepared by laser ablation in liquid are investigated. These parameters play an important role in the

* Corresponding author. Tel.: +20 1113370399.
E-mail address: kelsayed@niles.edu.eg (K.A. Elsayed).

0030-3992/$ - see front matter © 2012 Elsevier Ltd. All rights reserved.
http://dx.doi.org/10.1016/j.optlastec.2012.06.004

formation of small and narrowly dispersed gold nanoparticles and the mechanisms of the nanoparticles growth.

2. Experimental setup

Gold nanoparticles were produced by laser ablation of a metal gold plate in pure water solution. As shown in Fig. 1, the gold metal plate of 3 mm thickness (>99.99%) was thoroughly washed with ethanol and deionised water to remove organic contamination. The cleaned target was placed at the bottom of a glass vessel filled with 50 ml of de-ionized water. The gold metal plate was kept at 15 mm below the liquid surface. The metal plate was irradiated with an output of the fundamental (1064 nm) or the second harmonic (532 nm) of Quanta-ray Nd:YAG laser operating at 20 Hz and 10 ns pulse width. The laser beam was focused by a plano-convex lens having a focal length of 50 mm or 100 mm. The spot size of the laser beam on the surface of the metal plate was adjusted to 0.6 mm in diameter, by changing the distance between the focusing lens and the metal plate. OPHIR-NOVA power meter was used to monitor the laser power. The ablation time was kept at 5 min. The laser beam was focused on the surface of the target and it was scanned by using a X–Y stage to avoid the craters on the surface of target. Upon irradiation of the laser beam, the solution gradually turned to wine red. The absorption spectrum of the solution was measured by a PG instrument Ltd., T80+ spectrometer. At least five different runs were accumulated on computer to obtain one spectrum. A transmission electron microscope (HTEM (JEOL 1200)) was employed to take the electron micrographs of the nanoparticles in the solutions studied. The solution containing gold nanoparticles was inserted in the bath of ultrasonicator for half of an hour and a drop of solution containing gold nanoparticles was placed on carbon coated grids and allowed to completely dry at room temperature. The diameters of more than 100 nanoparticles visible on a given micro graph were directly measured and the distribution of the particle diameters (size distribution) was obtained.

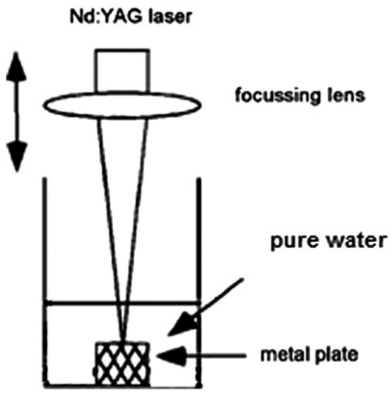

Fig. 1. Schematic diagram of experimental setup.

3. Results and discussion

3.1. Effect of laser energy

In this section, the influences of laser fluence on the size distribution of the gold nanoparticles and their optical properties are investigated. The gold nanoparticles were prepared at various laser energies output (10, 20, 30, 40, 50, 100, 150, 200, 250 mJ/pulse), the corresponding laser fluences were (4, 7, 11, 14 18, 35, 53, 70, 88 J/cm^2). The uncertainty of the pulse laser energy measurements was 5%. The ablation time in each case was 5 min. The laser fluence is divided into three regions, low fluence (4 J/cm^2), intermediate fluence (7–35 J/cm^2) and high fluence (53–88 J/cm^2). There are three different laser ablation mechanisms in these three regions that will be discussed in the following sections.

3.1.1. At low laser fluence (4 J/cm^2)

In the low fluence region, the target is heated, but due to the strong confinement of the liquid at the surface, the vaporization rate is strongly restricted and no plume is formed. In the absence of a vapor plume, the hot target remained in contact with water promoting the oxidation of the nanoparticles [16–18]. The reaction begins with the oxidation of the molten target surface by oxygen splitting of water molecules at the hot target so the nanoparticle hydroxide occurs on the target surface. The gold hydroxide material on the surface then desorbs from the hot target surface and diffuses into the water. It is not aggregated due to their negative charge. Therefore, the average size of produced gold nanoparticles is small as in Fig. 2. The average size is 6 nm as shown in Fig. 2; the particles are small and have spherical shape with a small yield. This is due to the negative charge on gold nanoparticles surface which prevent them from aggregation and their yield is small due to the presence of water at the surface of the target which restricts their growth as explained before.

3.1.2. Intermediate fluence (plume mixing zone) (7–35 J/cm^2)

At this stage the plume develops more slowly and is limited to a size much smaller than in a gas atmosphere. The large pressure in the confined vapor plume results in an expansion beyond the equilibrium point and the internal plume pressure equal the hydrostatic pressure of the liquid. Due to the difference between the pressure inside and outside the plume, the plume starts to decrease until it collapses. The particles become suspended in the solution as a direct result of the previous mentioned reason.

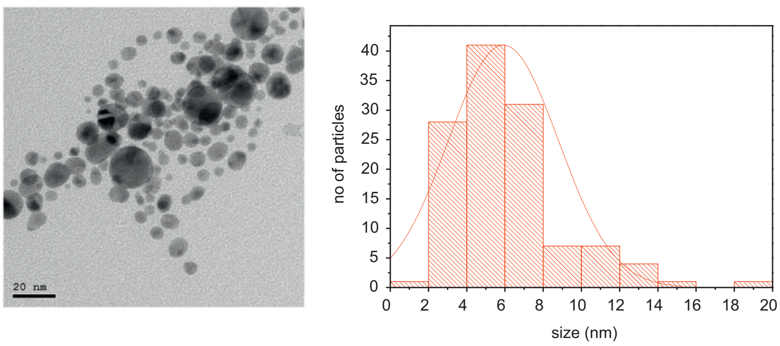

Fig. 2. TEM micrograph and histogram of gold nanoparticles prepared at 4 J/cm^2.

At low laser fluence the gold nanoparticle size decreases when the laser fluence increases while at high fluences region, the gold nanoparticle size increases when the laser fluence increases. The nanoparticles fall into two distinct size distributions mainly attributed to: (1) Target surface vaporization (2) Explosive ejection of molten droplets directly from the target [17,18]. The surface vaporization was discussed before. The explosive ejection occurs when the temperature approaches the thermodynamic critical temperature, where the thermal fluctuations are amplified and the rate of homogenous bubble nucleation rises dramatically. Consequently, the target undergoes rapid transition from superheated liquid to a mixture of vapor and equilibrium liquid droplet. At this fluence, the momentum of plume allows it to expand further into the liquid, increasing the plasma life time and this results in an increase in the amount of screened laser light [19,20].

Fig. 3(a)–(e) shows that the average size of gold nanoparticles prepared in pure water at 7, 11, 14, 18, 35 J/cm^2 are 14, 13, 13, 12 and 8 nm respectively. As it is shown the average size decreases with increasing laser fluence. From TEM micrographs it is found that, as laser power increases, the particles become homogenous and have spherical shape, also the concentration increases until it takes critical size at 35 J/cm^2, the particles appear as diffused particles. The decrease in the average size of gold nanoparticles can be attributed to large fluence. This will excite the gold nanoparticles in the solution, the photon energy is readily converted to the internal modes of the nanoparticles as during a single laser pulse, one gold nanoparticle is considered to absorb consecutively more than one thousand photon and its temperature rises significantly so that the nanoparticle starts to fragment [17,18]. After the single laser pulse diffused into the solution, the temperature of nanoparticles returns to room temperature before the next one arrives. The heating and cooling of nanoparticles occur in every laser pulse.

3.1.3. *High fluence (plasma etching) (53–88 J/cm^2)*

At high fluence, laser power is absorbed in the liquid and reached the target resulting in a material removal by reactive sputtering rather than direct laser ablation. As the intensity of laser in the presence of ablated material in water decreases, the amount of the light to the target tends to zero. Therefore, the

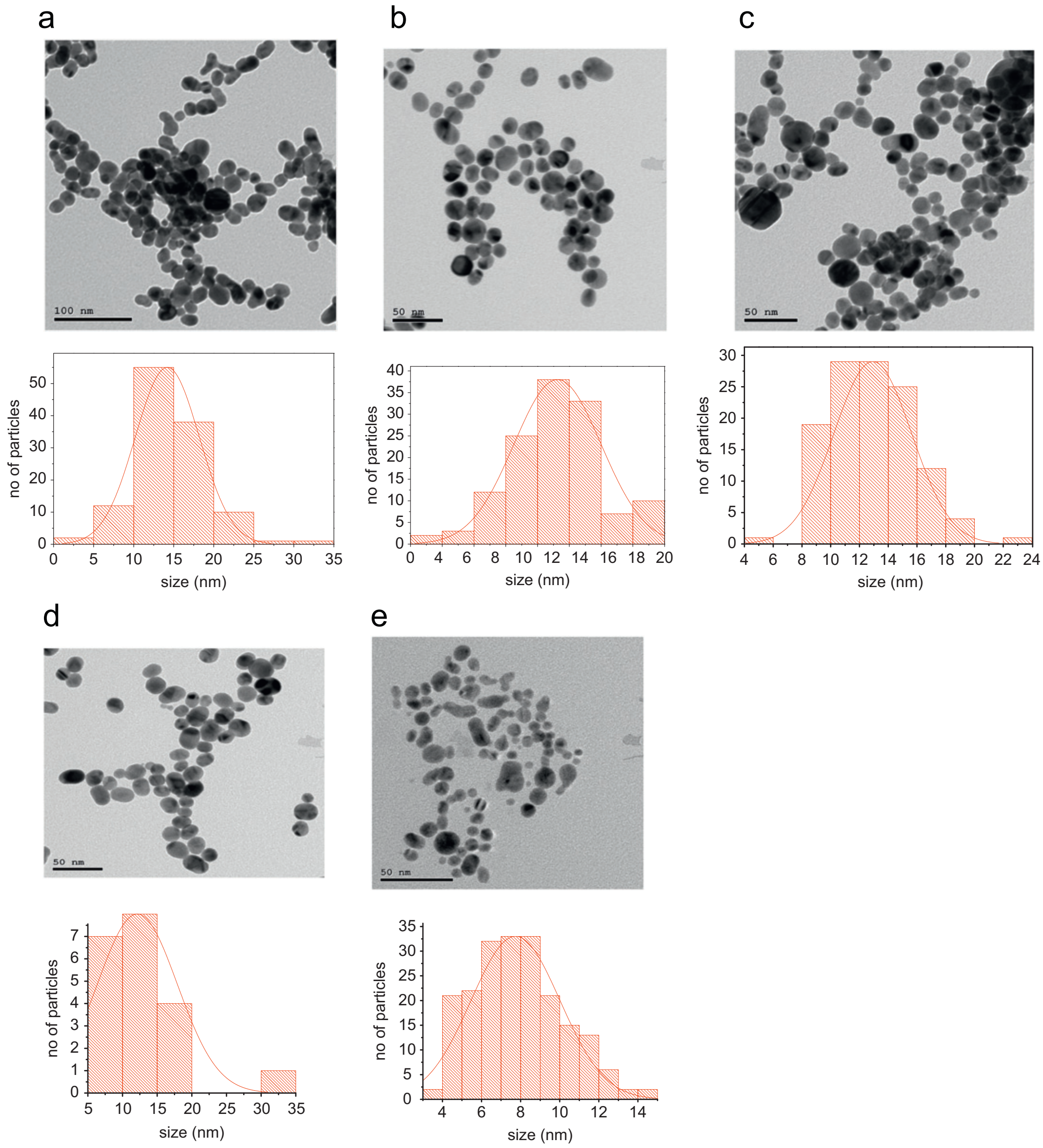

Fig. 3. (a–e): TEM micrographs and their histograms of gold nanoparticles prepared at various laser fluences of 7, 11, 14, 18 and 35 J/cm^2 respectively.

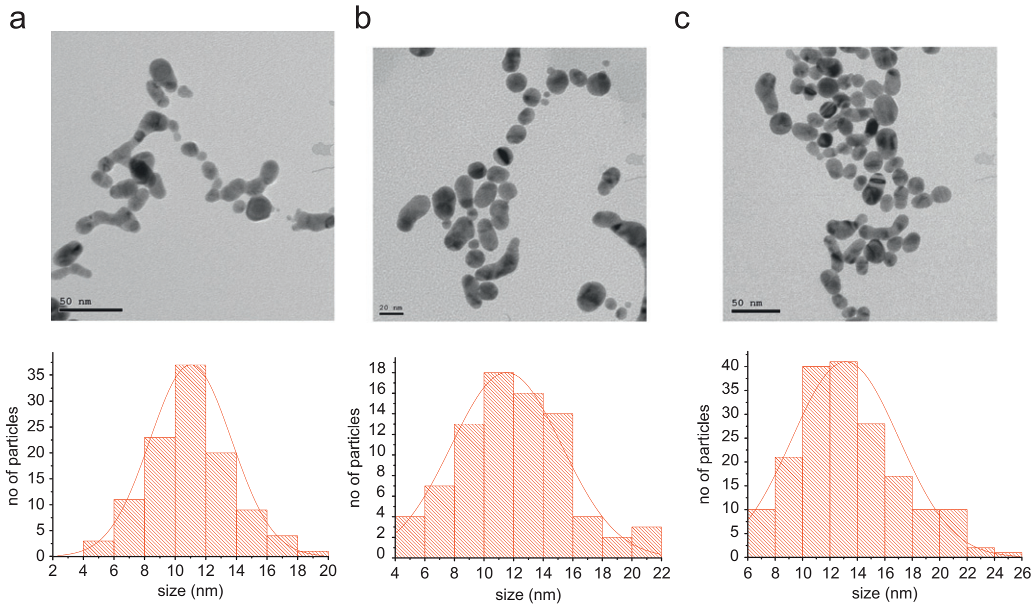

Fig. 4. (a–c): TEM micrographs and histogram of gold nanoparticles prepared by using pure water in 53, 70 and 88 J/cm^2 respectively.

plasma formation in the water creates a cavitation bubble that expands and then collapses, driving highly energetic species into target surface [17]. In this region the average size of gold nanoparticles begins to increase again as shown in Fig. 4(a)–(c). The figure shows the average size of gold nanoparticles that were prepared in pure water at fluences of 53, 70 and 88 J/cm^2 is 11, 13 and 14 nm respectively. It is observed that when laser fluence exceeds a certain value (above 35 J/cm^2), the average size and concentration begin to increase and the shape of prepared gold nanoparticles begins to take the spherical shape again after the diffused shape. When it is prepared at 35 J/cm^2, the gold nanoparticles reach their critical size, small fragments such as gold atoms and small aggregates resulting from photo fragmentation are dispersed in solution. Therefore, the nanoparticles present in the solution grow by attracting these small fragments.

The fragmentation rate must increase with increasing laser fluence because the internal energy of irradiated nanoparticles increases. On the other hand, the aggregation rate increases with the increase of the concentration of the small fragments. After the laser is switched off, the fragmentation is terminated and only the aggregation proceeds until the gold atoms and small fragments are consumed. The fragmentation rate of each nanoparticle decreases because the absorption coefficient per atom decreases with its diameter. On the other hand, the aggregation rate increases because the concentration of the small fragments increases. Therefore, the minimum diameter is realized when the rate of fragmentation is equal to that of the aggregation [17].

From the above discussion, the average size decreases as the laser fluence increases until it reaches the critical size then it begins to increase again as shown in the reported data in Table 1 and Fig. 5. The absorbance spectra are investigated to indicate the concentration and size distribution of the prepared gold nanoparticles. The position and height of the peak in the optical absorption spectrum of gold nanoparticles depend on the shape, size and the yield of the obtained particles. This is enhanced by the results of TEM. Fig. 6 shows that as the laser fluence increases, the height of the plasmon peak increases. This indicates the increase in the concentration of nanoparticles, until reaching the critical size (at 35 J/cm^2) then the absorption coefficient of gold nanoparticles starts to decrease and their shape starts to diffuse and lose their spherical shape. The nanoparticles absorb

Table 1
The dependence of the average particle size and laser fluence in water.

Laser fluence (J/m^2)	Average size (nm)	Size distribution (nm)
7	14	2–32
11	13	5–20
14	13	5–23
18	12	5–22
35	8	3–15
53	11	4–20
70	13	4–21
88	14	6–25

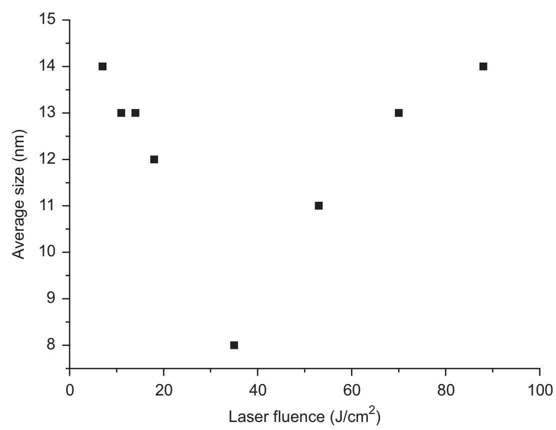

Fig. 5. The variation of Gold nanoparticles prepared in de-ionized water with laser fluence.

no more and, thus, are no more fragmented. The small red-shift in the plasmon peak assures the decrease in the average size of gold nanoparticles. As the laser power increases, the plasmon peak becomes narrower indicating that the particles have a homogenous distribution. The absorbance spectra obtained at high fluence is shown in Fig. 7. At high laser fluence (53–88 J/cm^2), the absorbance shows that the height of Plasmon peak increases with increasing laser fluence indicating the increase in the concentration of gold nanoparticles. As the laser fluence increases, the peak width decreases with a small blue-shift in the plasmon peak due to the small increase in the size of the gold nanoparticles. These results are matched with those obtained from TEM micrographs.

The effect of laser fluence on the mean size, size distribution and optical properties of gold nanoparticles were investigated for aqueous solution of (60:40); (water:ethanol) ratios with other experimental parameters kept the same. The average size of the prepared gold nanoparticles is 9, 13, 11, 10, 10, 9, 8, 7 and 9 nm at laser fluences 4, 7, 11, 14, 18, 35, 53 and 88 J/cm^2 respectively. The nanoparticles critical size was obtained in 40% ethanol at 53 J/cm^2 while that prepared in deionised water reaches critical size at 35 J/cm^2. This can be explained as the gold nanoparticles in ethanol are more aggregated than those prepared in water. This is due to the H atom in water having electron negativity lower than the C atom in ethanol so the water has more dissociated OH^- group than that of ethanol. In other words, water creates strong electrical double layer around the nanoparticles due to electrical interaction between species in plume and this layer. The growth becomes restricted during ablation resulting in small gold nanoparticles formation in water. Low polarity of ethanol molecules lead to weak electrical double layers, therefore the growth in particle size is enhanced with strong agglomeration. Accordingly, the gold nanoparticles prepared in ethanol required higher fluence to reach their critical size. The relation between laser fluence and average size of gold nanoparticles prepared at 40% ethanol is summarized in Table 2 and Fig. 8

3.2. The effect of wavelength

The effect of laser ablation has been expressed in terms of the amount of ablated Au as determined by the area of surface plasmon peak of the resulting gold nanoparticles [21]. Laser ablation efficiency increases as the laser wavelength increases. Consequently the efficiency of laser ablation at 1064 nm is higher than the laser ablation at 532 nm as shown in Fig. 9.

Table 2
Relation between average sizes of gold nanoparticles samples prepared in 40% ethanol and the laser fluence.

Laser fluence (J/cm^2)	Average size (nm)	Size distribution (nm)
4	13	4–35
7	11	6–18
11	10	8–15
14	10	2–14
18	9	7–15
35	8	4–11
53	7	6–17
70	9	4–17

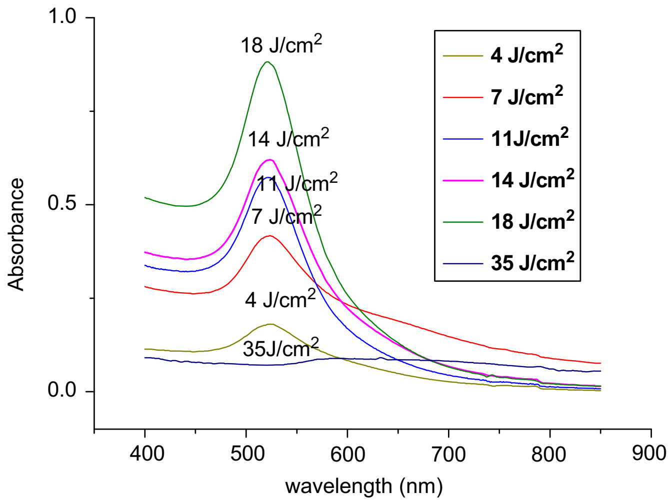

Fig. 6. The absorbance spectra of gold nanoparticles prepared in pure water at various fluences (low and intermediate fluence).

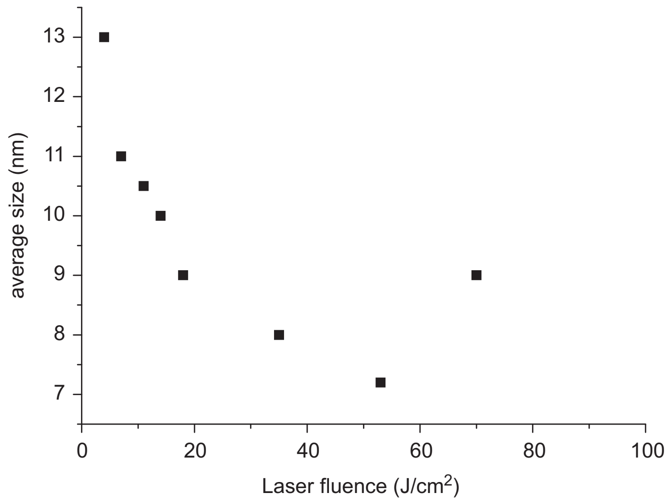

Fig. 8. The variation of the average size of gold nanoparticles prepared in 40% ethanol with laser fluence.

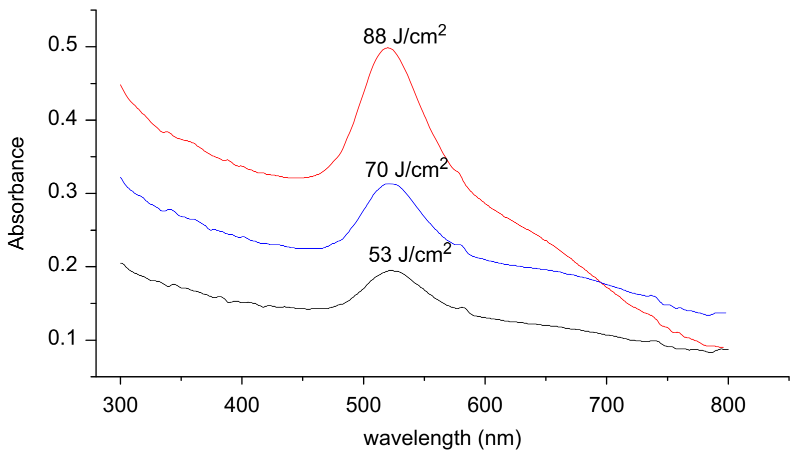

Fig. 7. The absorbance spectra of gold nanoparticles prepared in pure water at high laser fluence.

From Fig. 9, the intensity of surface plasmon peak of gold nanoparticles prepared at 1064 nm is higher than that prepared at 532 nm, which indicated that the amount of gold nanoparticles prepared at 1064 nm is higher than that prepared at 532 nm. From TEM micrographs, shown in Fig. 10, the nanoparticles distribution of 1064 are more homogenous and the average size of gold nanoparticles prepared at 532 nm is smaller than that prepared at 1064 nm.

The average size of the gold nanoparticles prepared at 532 nm is smaller than the gold nanoparticles prepared at 1064 nm. This could be attributed to two factors: the value of the absorption coefficient and the photon energy. The value of the absorption coefficient of bulk gold is higher in the case of 1064 nm. The photon energy of 532 nm is higher than the photon energy of 1064 nm. This leads to the fragmentation of gold nanoparticles prepared at 532 nm and consequently results in the generation of a smaller size of gold nanoparticles.

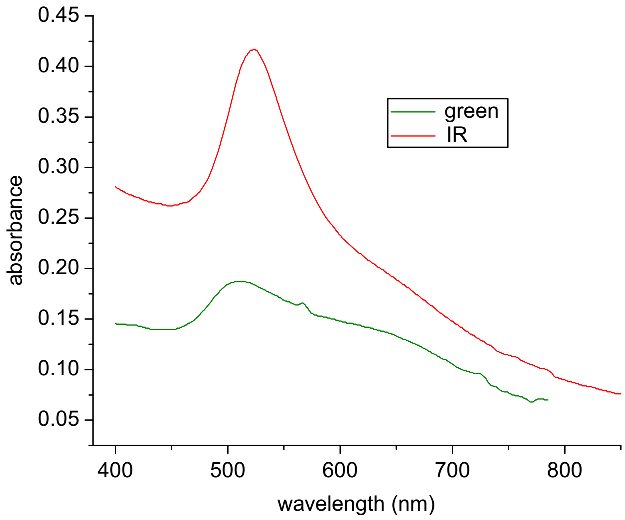

Fig. 9. The absorbance spectrum of gold nanoparticles prepared in de-ionized water at 1064 and 532 nm.

3.3. Effect of focusing conditions on the gold nanoparticles

The focusing conditions is one of the important parameters that plays an important role in the formation of small and narrowly dispersed gold nanoparticles. Gold nanoparticles were prepared by varying the focusing conditions at gold–water interface. The target positioned and ablated at focus, above focus and below focus conditions of the laser beam. This is not only changing the fluence but also change the degree of ionization of surrounding liquid medium, hence, it is interesting to study its implications on synthesized nanoparticles especially beyond the focal volume.

The Q-switched Nd:YAG laser at fundamental wavelength was focused by a 5 cm focal length lens onto a gold target placed inside liquid cell filled with distilled deionized (conductivity $< 1\ \mu\Omega\ cm^{-1}$) water. The laser (pulse width = 6 ns) was operated at the repetition rate of 10 Hz and laser pulse energy of 50 mJ. The ablation time was kept at 5 min.

The laser ablation from the surface of the target due to the incident intense laser beam led to plasma formation which interacts with the surrounding water layer. The target was ablated at different focusing by changing the position of the lens by means of a micrometer (μm) screw attached with the lens mount. For each focusing condition the spot size on the target was measured by exposing it to a single shot laser for all three geometries. The exposed areas were subjected to SEM. The spot size at above, at and below focus were 600, 150 and 500 μm

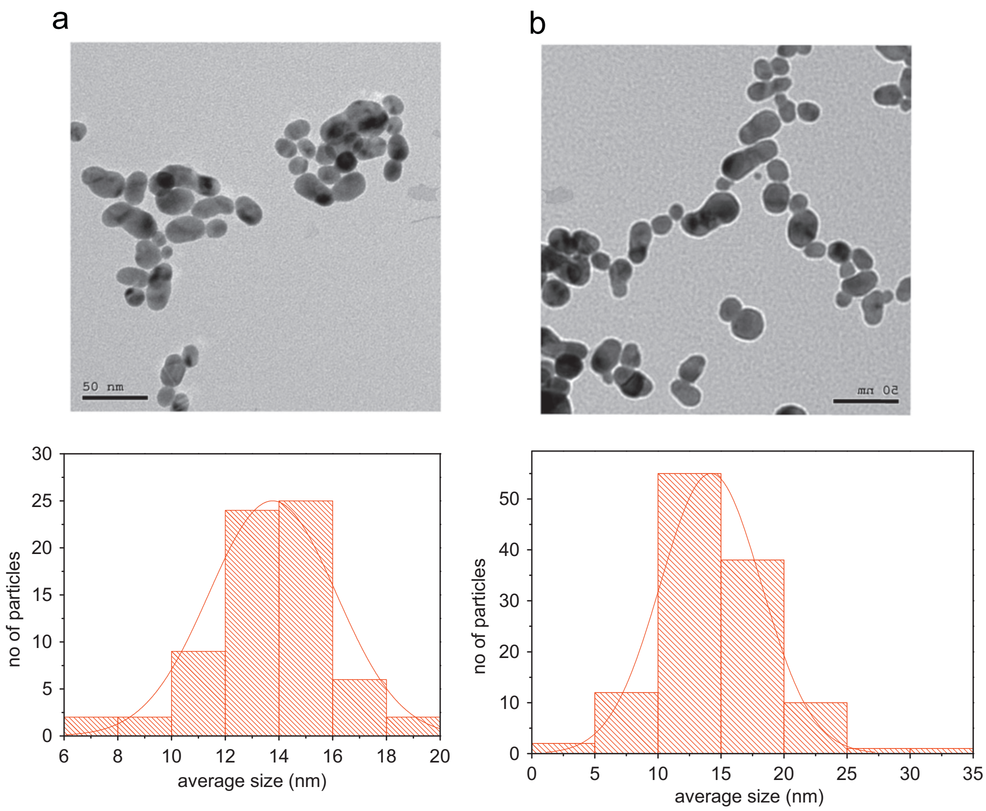

Fig. 10. The TEM micrograph and histogram of gold nanoparticles prepared at (a) 532 nm and (b) 1064 nm.

respectively. The estimated laser fluence was 17 J/cm^2, 280 J/cm^2 and 25 J/cm^2 for above, at and below focus conditions respectively. The prepared colloidal solutions containing nanoparticles obtained via ablation at different focusing conditions were taken for recording the UV–visible (UV–vis) spectra and the size distribution of the nanoparticles using TEM.

The average size of the obtained gold nanoparticles prepared at different positions "above focus", "at focus" and "below focus" are summarized in Table 3. The size of the gold nanoparticles prepared "above focus" with a lens of 5 cm is 8 nm. The yield is small and the particles are diffused. This may be due to the low fluence and water breakdown does not take place [17]. At this region, the target is heated and due to the strong confinement of the liquid at the surface and the vaporization rate is strongly restricted and no plume is formed [18]. The average particle size at "focus" is 9 nm. The particles have a spherical shape and also are agglomerated. This can be explained as follows: when the ablation takes place at the focus, the plasma pressure, temperature and density increase more than in the defocusing condition. High temperature of plasma temperature excites, ionizes and dissociates the surrounding water layer, the nucleation starts directly. The high density plasma increases the molecular interaction and particles' growth resulting in an increase in the particles' size as it was observed. When laser is switched off, plasma cooling and recombination take place, the pressure and temperature will be reduce but the particle growth continues until a certain value above which it ceases.

The average size of the gold nanoparticles prepared at "below focusing" decreases down to 7 nm. In this case, most of the fluence at the focal region is absorbed by the water and the fluence that reached the target was reduced. In this case the screening effect of laser light plays a significant role, therefore the laser energy reaching the target is low [18].

The same behavior was noticed when using a larger focal length of 10 cm but the average size of the obtained gold nanoparticles increases as the focal length increases. The obtained results are summarized in Table 3.

Another parameter of the focusing conditions that affect the shape and size distribution of the gold nanoparticles is the focal length. The minimum diameter of laser beam spot changes with changing the focal length of the used lens. This in turns changes the laser fluence and hence produces gold nanoparticles with different shapes and sizes. Laser plasma is known to be highly dependent on the laser fluence at the surface [18].

The spot size on the target was measured by exposing it to a single shot. The exposed areas were subjected to SEM. The spot size was about 150, 300 and 600 μm for 5, 10 and 20 cm focal length, respectively. The fluence decreases with increasing focal length, as a result, the average size increases and the yield of the obtained particles also increases. At small focal length ($f=5$ cm), very small and hot plasma was produced due to high fluence (280 J/cm^2) that is localized at the focal point thereby the average size of the produced gold nanoparticles is small and have spherical shape with larger yield. This may be due to that the absorption of irradiance, in liquid, reaches the target and the material ablation takes place by reactive sputtering [14].

Table 3
Variation of the target position and the average particle size.

	Target position	Average size (nm)	Size distribution (nm)
$F=5$ cm	Above focusing	8	4–14
	At focusing	9	4–18
	Below focusing	7	3–45
$F=10$ cm	Above focusing	9	5–15
	At focusing	10	5–19
	Below focusing	8	3–17

Table 4
The relation between the average particle size and laser irradiance.

Focal length (cm)	Laser fluence (E/A) (J/cm^2)	Average size (nm)	Size distribution (nm)
5	280	9	4–17
10	70	10	4–20
20	18	18	4–50

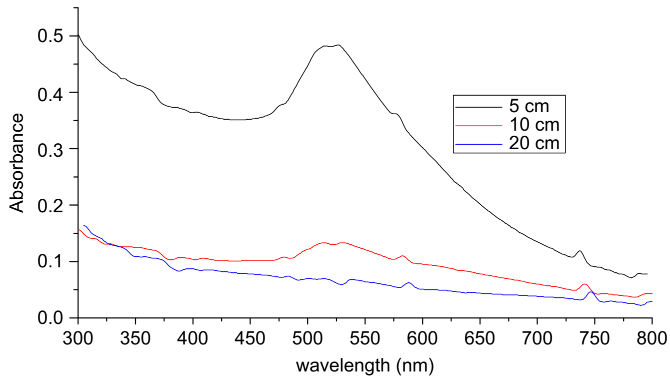

Fig. 11. Absorbance spectra of gold nanoparticles prepared in pure water at various focal lengths.

The gold nanoparticles prepared at focal length ($f=10$ cm) at laser fluence is lower (70 J/cm^2), and the obtained particles are enlarged with broader distribution. This is because the laser pulses produce small fragments above the sample, the next pulse is partially scattered by these small particulates. Consequently, too small portion of the power reaches the target surface of the target. At focal length ($f=20$ cm), the average size of gold nanoparticles is larger than that obtained at focal lengths 5 and 10 cm as the laser fluence became smaller (18 J/cm^2) due to longer focus depth of the laser beam in spite of the existence of small particulates. The irradiance of laser beam is scattered and very small amount of the fluence reaches the target resulting in a small yield with a large average size and broadened distribution. Table 4 summarized the obtained results.

Fig. 11 shows the absorbance spectra of gold nanoparticles prepared at focal lengths of 5, 10, and 20 cm, the height of peak decreases with the increase of the focal length which contributed to the small yield obtained. Also, there is a shift to the longer wavelength with the increase of the focal length assigned due to the increase of the average size of gold nanoparticle. These results agree with those observed in TEM [22,23].

4. Conclusion

Gold nanoparticles were prepared by laser ablation in water and ethanol solution.

The control of the gold nanoparticles size and hence colloidal properties is possible using laser parameters such as laser fluence and wavelength as well as varying the focusing conditions. These parameters play an important role in the formation of small and narrowly dispersed gold nanoparticles and the mechanisms of the nanoparticle growth.

As the laser fluence increases, the size of gold nanoparticles prepared in de-ionized water decreases until they reached their critical size (8 nm at 35 J/cm^2) below which the particle became insensitive to the laser energy. As the energy increases above this value the nanoparticles begin to agglomerate again and the size increases. The same trend was noticed in 40% ethanol solution but the critical size was obtained at higher fluence (7 nm at 53 J/cm^2) due to higher agglomeration. Smaller size distribution and yield was obtained at shorter wavelength of 532 nm. The focal length and the position of the samples both have a notable affect on the shape and size distribution of the gold nanoparticles. A small size gold nanoparticle in the range of 7 nm can be generated at shorter focal length when placing the target below the focus. Small size and narrow distribution of the gold nanoparticles prepared by laser ablation can be controlled by optimizing the laser parameters and focusing conditions.

References

[1] Alanazi FK, Radwan AA, Alsarra IA. Saudi Pharmaceutical Journal 2010;18:179.
[2] Yoo EJ, Li T, Park HG, Chang YK. Ultramicroscopy 2008;108:1273.
[3] Shakibaie M, Forootanfar H, Mollazadeh-Moghaddam K, Bagherzadeh Z, NafissiVarcheh N, Shahverdi AR, et al. Biotechnology and Applied Biochemistry 2010;57:71.
[4] Maliszewska I, Aniszkiewicz L, Sadowski Z. Acta Physica Polonica A 2009;116:163 S–.
[5] Mukherjee P, Senapati S, Mandal D, Ahmad A, Khan MI, Kumar R, et al. ChemBioChem 2002;3:461.
[6] Ebenau A. Mannheim, 28–29 October 2002 (BASF Future Business GmbH, Ludwigshafen, press release; 2002.
[7] Alt V, Bechert T, Steinrucke P, Wagener M, Seidel P, Dingeldein E, et al. Biomaterials 2004;25:4383.
[8] Tartaj P, Morales M, Veintemillas S. Journal of Physics D: Applied Physics 2003;36(13):R182–97.
[9] Fujiwara H, Yanagida S, Kamat PV. Journal of Physical Chemistry B 1999;103:2589.
[10] Hodak JH, Henglein A, Giersig M, Hartland GV. Journal of Physical Chemistry B 2000;104:11708.
[11] Yeh Y-H, Yeh M-S, Le Y-P. Chemistry Letters 1998:1183.
[12] Petersen S, Barcikowiski S. Journal of Physical Chemistry C 2009;113:19830.
[13] Kabashim AV, Munier M. Journal of Applied Physics 2003;94:7941.
[14] Tsuji T, Iryo K, Wafanabe N, Tsuji M. Applied Surface Science 2002;202:80.
[15] Sylrestre Jp, Kabashim AV, Sacher E, Munier M. Applied Physics A 2005;80:753.
[16] Tarasenko NV, Butsena AV, Nevara EA, Savastenko NA. Applied Surface Science 2006;252:4439.
[17] Nichols WT, Sasaki T, Koshizaki N. Journal of Applied Physics 2006;100:114912.
[18] Nichols WT, Sasaki T, Koshizaki N. Journal of Applied Physics 2006;100:114913.
[19] Kima HJ, Bangband IC, Jun Onoe. Optics and Lasers in Engineering 2009;47:532.
[20] Dolgaev SI, Simakin AV, Voronov VV, Shafeev GA, Verduraz FB. Applied Surface Science 2002;186:546.
[21] Šmejkal P, Pfleger J, Vlčková B, Dammer O. Journal of Physics: Conference Series 2007;59:185.
[22] Natha A, Lahaa SS, Khare A. Applied Surface Science 2011;257:3118.
[23] Bulatov V, Xu L, Schechter I. Analytical Chemistry 1996;68:2966.